

marker. Appropriate probe position resulted in the core region becoming clearly visible while the outer regions of the vortex remained unmarked. A laser sheet aligned normal to the wing surface highlighted the smoke-filled core. Kerosene smoke and  $\text{TiCl}_4$  were used simultaneously in the photographs in Figs. 3b and 3c, with the laser sheet aligned parallel and normal, respectively, to the vortex core. These photographs again illustrate the effectiveness of an appropriately positioned  $\text{TiCl}_4$  injection probe in placing tracer particles into the core region.

These preliminary observations indicate several interesting flow features. The core appears to maintain a more or less constant diameter upstream of breakdown. Similar results can be seen in the water-tunnel studies by Erickson<sup>3</sup> and Werle.<sup>6</sup> Because the probe sweeps over the wing showed no sign of particle entrainment of the outer vortex by the core region and the core fluid itself shows no apparent sign of exiting from that region, this would seem to indicate a more or less steady core flow and no mixing with the surrounding vortical flow.

Furthermore, previous arguments indicating the particle-scarce core region to be a result of the high circumferential velocity, or the migration of particles to a pressure matching region between the inner and outer flow regimes, seem questionable, because no particle, once in the core, was observed to exit from that region. It is more likely that the core fluid originates from the streamlines that pass through a small region near the apex. Unless the particle concentration in the core fluid is high at the beginning, acceleration and expansion of the core fluid may dilute the particle concentration, making the core fluid less effective in scattering light and resulting in a comparatively dark region.

### Concluding Remarks

The possibilities with the particle injection scheme should not be overlooked, especially with respect to LDV, which requires tracer smoke particles for its operation. With the proper injection techniques, the problem that plagues most LDV measurements on delta wings, namely, the lack of particles in the vortex core, can be eliminated. This method can help other localized flowfield studies, especially those void of particles by standard flow visualization methods. The vortex core region is only one application that can be investigated. Vortex trajectory mapping can also be accomplished by this method and, in particular, multiple vortex interaction.

These initial wind-tunnel investigations have indicated that the vortex core over a flat delta wing appears to maintain a more or less constant diameter until breakdown. The core may also be maintaining a constant velocity up to the breakdown point, as suggested by the very little mixing seen to occur between the core and the outer flow.

### Acknowledgments

The authors wish to express their thanks to all those involved with the experiments, especially Mr. James Carey and Mr. Christopher Knors of the University of Notre Dame Chemistry Department for their advice on handling air-sensitive materials. The photos shown in Fig. 1 are from a cooperative NASA Ames/University of Notre Dame study of vortex flow with Garry Erickson. Support by the NASA Ames research Grant NCA2-162 is also gratefully acknowledged.

### References

- <sup>1</sup>Nelson, R.C., Payne, F.M., and Ng, T.T., "Visualization of Vortex Breakdown on a Delta Wing" *Flow Visualization IV*, edited by C. Veret, Hemisphere, New York, 1987, pp. 431-436.
- <sup>2</sup>Payne, F.M., "The Structure of Leading Edge Vortex Flows Including Vortex Breakdown," Ph.D. Dissertation, University of Notre Dame, IN, May 1987.
- <sup>3</sup>Erickson, G.E., "Vortex Correlation," AFWAL-TR-80-3143, Jan. 1981.
- <sup>4</sup>Verhaagen, N.G., "An Experimental Investigation of the Vortex Flow Over Delta and Double-Delta Wings at Low Speed," AGARD-

CP-342, April 1983.

<sup>5</sup>Malcolm, G.N. and Nelson, R.C., "Comparison of Water and Wind Tunnel Flow Visualization Results on a Generic Fighter Configuration at High Angles of Attack," AIAA Paper 87-2423, 1987.

<sup>6</sup>Werle, H., "Flow Visualization Techniques for the Study of High Incidence Aerodynamics," AGARD-LSP-121, Feb. 1982, pp. 3-1-3-36.

<sup>7</sup>Simmons, L.F.G. and Dewey, N.S., "Photographic Records of Flow in the Boundary Layer," Reports and Memoranda of the Aeronautical Research Council, No. 1335, London, 1931.

<sup>8</sup>Freymuth, P., Bank, W., and Palmer, M., "Use of Titanium Tetrachloride for Visualization of Accelerating Flows Around Airfoils," *Flow Visualization III*, edited by W.J. Yang, Hemisphere, New York, 1985, pp. 99-105.

<sup>9</sup>Mueller, T.J., Brendel, M., and Schmidt, G.S., "Visualization of the Laminar Separation Bubble at Low Reynolds Numbers," *Flow Visualization IV*, edited by C. Veret, Hemisphere, New York, 1987, pp. 359-364.

## Drag Reduction Factor Due to Ground Effect

Young B. Suh\* and Cyrus Ostowari†  
Texas A&M University, College Station, Texas

### Introduction

NUMEROUS investigators<sup>1-7</sup> have studied and experimented with ground interference on the aerodynamic characteristics of wings. The general trend of this effect is an increasing lift-curve slope and a decreasing induced drag as the distance between the wing and ground is reduced. In this Note, we derive a theoretical working formula of this effect and compare it with existing formulas and experimental data.

The drag equation of an aircraft can be written as  $C_D = C_{D0} + KC_L^2$ , where  $K = (\pi R A e)^{-1}$ ,  $R$  (aspect ratio)  $= (2s)^2/A_s$ ,  $A_s$  = span area. Here,  $s$  and  $e$  are the half-span and Oswald's wing efficiency, respectively. Usually, there are two ways to incorporate the ground effect in this drag equation, i.e.,

$$C_D = C_{D0} + \Phi KC_L^2, \quad 0 < \phi < 1 \quad (1a)$$

$$C_D = C_{D0} + C_L^2/(\pi e A_{\text{eff}}) \quad (1b)$$

where  $A_{\text{eff}}$  is the effective aspect ratio resulting from the inclusion of the ground effect. These two are equivalent through the relation  $A_{\text{eff}} = R/\Phi$ .

There exist several theoretical expressions of the drag reduction factor  $\Phi$ , namely Prandtl's<sup>8</sup>

$$\Phi(\text{Prandtl}) = \frac{8.72 + 0.1s/h}{7.4 + 2.1s/h}, \quad 2 \leq s/h \leq 15$$

and McCormick's<sup>9</sup>

$$\Phi(\text{McCormick}) = \frac{(8h/s)^2}{1 + (8h/s)^2}$$

However, in the present discussion, this factor has been derived rather differently, as shown below.

Because of the presence of the solid wall, the simplified horseshoe vortex system of an aircraft will accompany its image vortex system reflected in the plane boundary (runway).

Received Oct. 29, 1987; revision received May 2, 1988. Copyright © American Institute of Aeronautics and Astronautics, Inc., 1988. All rights reserved.

\*Research Assistant, Mechanical Engineering Department.

†Associate Professor, Aerospace Engineering Department.

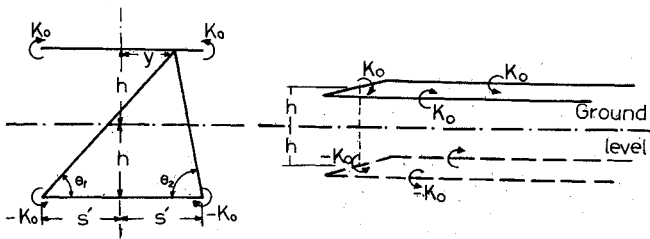


Fig. 1 Simplified horseshoe vortex and its image vortex system reflected in the plane wall (runway).

The situation is depicted in Fig. 1. The original elliptic loading is replaced by an equivalent rectangular loading with the same height  $K_0$ , but reduced span  $2s' = \pi s/2$ , i.e., the length of the equivalent bound vortex. The induced upwash due to the image trailing vortex system at the span location will be<sup>10</sup>

$$\Delta w_1 = \frac{K_0}{4\pi} \left( \frac{s' + y}{r_1^2} + \frac{s' - y}{r_2^2} \right)$$

The lift gain of the span length  $\delta y$  is  $\delta l = \rho U K_0 \delta y$ , which yields the induced drag reduction,  $\delta d_v = \delta l \Delta w_1 / U = \rho K_0 \delta y \Delta w_1$ . The total drag reduction is

$$\Delta D_v = \int_{-s'}^{s'} \delta d_v = \frac{\rho K_0^2}{4\pi} \ln \left[ 1 + \left( \frac{\pi s}{4h} \right)^2 \right]$$

where the relations  $r_1^2 = 4h^2 + (s' + y)^2$  and  $r_2^2 = 4h^2 + (s' - y)^2$  have been used. Making use of the Kutta-Joukowski theorem,  $L = \rho U K_0 2s' = \rho U K_0 \pi s/2$ , we finally obtain

$$\Delta D_v = \frac{\rho C_L^2 U^2 A_s^2}{4\pi^3 s^2} \ln \left[ 1 + \left( \frac{\pi s}{4h} \right)^2 \right] \quad (2)$$

Therefore, we write the net aerodynamic drag as  $D_A = \frac{1}{2} \rho U^2 A_s C_D - \Delta D_v$ . When this equation is put into the form of Eq. (1a), i.e.,

$$D_A = \frac{1}{2} \rho U^2 A_s (C_{D0} + \Phi K C_L^2)$$

we finally arrive at the following drag reduction factor;

$$\Phi = 1 - \frac{2e}{\pi^2} \ln \left[ 1 + \left( \frac{\pi s}{4h} \right)^2 \right] \quad (3)$$

It is easily seen that  $\lim_{h \rightarrow \infty} \Phi = 1$  (out-of-ground effect) as should be the case. Here, we notice that our expression [Eq. (3)] differs from those preceding in that Eq. (3) contains the explicit dependence on  $e$ , Oswald's wing efficiency as well as  $s/h$ . This dependence is experimentally supported by the earlier wind-tunnel test by Furlong and Boilech,<sup>7</sup> in which these investigators found that effects of sweepback and taper ratio show different characteristics from unswept and rectangular wings. Naturally, these wing parameters could lump into some form of the wing efficiency,<sup>11</sup> for instance, Weissinger planform efficiency factor  $e'$ .<sup>12</sup> It should be understood that the Oswald wing efficiency  $e$  is the measure of departure from the ideal elliptical loading in the portion of the induced drag.

### Results and Discussion

Figure 2 compares the foregoing three expressions of  $\Phi$  along with experimental data obtained by Fink and Lastinger,<sup>13</sup> in which the notion of  $A_{\text{eff}}$  was employed. As are shown in Fig. 2, the McCormick factor underestimates the ground effect, whereas Prandtl factor somewhat overestimates the effect in the same  $s/h$  range.

The present reduction factor [Suh-Ostowari, Eq. (3)] generally agrees with the wind-tunnel test when  $e \sim 0.85$  and  $0.9$  are

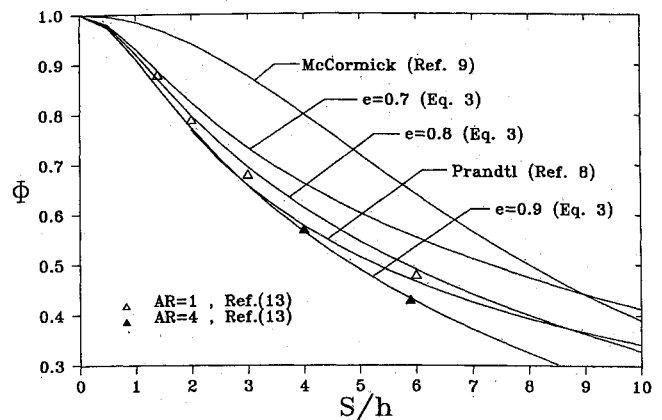


Fig. 2 Effect of ground on the drag reduction factor  $\Phi$ .

assumed for  $AR = 1$  and  $4$ , respectively. These values of  $e$  are quite feasible in the absence of wing/fuselage interference and for the unswept, untapered wings used in the experiment.<sup>13</sup> As shown in Fig. 2, the ground effect is more pronounced for wings of higher  $e$  (Oswald's wing efficiency), i.e., smaller  $\Phi$ . Equation (3) generally agrees well with the results of wind-tunnel test for all practical  $s/h$  ranges ( $s/h < 7.5$ ). It can be noticed that at zero angle of attack, the lift coefficient  $C_L$  nearly remains unchanged as  $s/h$  varies.<sup>13</sup> Consequently,  $C_L$  appearing in Eqs. (1a) and (1b) will be the same as that without ground effect if angle of attack is close to zero.

We conclude our discussion by noticing that Eq. (3) should provide a useful guide in the analysis of takeoff and/or landing performance.

### Acknowledgment

The authors are grateful to Prof. Thomas U. McElmurry of the Aerospace Engineering Department at Texas A&M for his unreserved willingness to discuss numerous topics in aerodynamics and performance.

### References

- Wieselsberger, C., "Wing Resistance Near the Ground," NACA TM 77, 1922.
- Reid, E. G., "A Full-Scale Investigation of Ground Effect," NACA Rept. 265, 1927.
- Pistolessi, E., "Ground Effect-Theory and Practice," NACA TM 828, 1937.
- Tani, I., Taima, M., and Simidu, S., "The Effects of Ground on the Aerodynamic Characteristics of a Monoplane Wing," Aeronautical Research Institute, Tokyo Imperial University, Tokyo, Rept. 156 (Vol. XIII, No. 2), 1937.
- Recant, I. G., "Wind-Tunnel Investigation of Ground Effect on Wings with Flaps," NACA TN 705, 1939.
- Katzoff, S. and Sweberg, H. H., "Ground Effect on Downwash Angles and Wake Location," NACA Rept. 738, 1943.
- Furlong, G. C. and Boilech, T. V., "Effect of Ground Interference on the Aerodynamic Characteristics of a 42° Sweptback Wing," NACA TN 2487, 1948.
- Prandtl, L., "Wing Theory," Bulletin of the Göttingen Scientific Society, 1919.
- McCormick, B. W., *Aerodynamics, Aeronautics and Flight Mechanics*, Wiley, New York, 1979, p. 420.
- Houghton, E. L. and Carruthers, N. B., *Aerodynamics of Engineering Students*, 3rd ed., Edward Arnold, 1984, p. 285.
- Nicolai, L. M., *Fundamentals of Aircraft Design*, Mets, Inc., 1984, Fig. 11-5.
- Furlong, G. C. and McHough, J. G., "A Summary and Analysis of Low Speed Longitudinal Characteristics of Swept Wings at High Reynolds Number," NACA Rept. 152d16, 1952.
- Fink, M. P. and Lastinger, J. L., "Aerodynamic Characteristics of Low-Aspect-Ratio Wings in Close Proximity to the Ground," NASA TN D-926, 1961.